The Small-Particle Response of an Optical Array Precipitation Probe

MICHAEL J. CURRY[1] AND ROBERT S. SCHEMENAUER

Atmospheric Environment Service, Downsview, Ontario, Canada M3H 5T4

(Manuscript received 6 June 1978, in final form 22 December 1978)

ABSTRACT

The response characteristics of an optical array precipitation spectrometer probe (PMS-OAP-200Y) have been studied in the laboratory using precision glass beads ejected from a specially constructed air gun. The low-end behavior of the probe is described in terms of a high-pass filter characteristic, which can be used to explain the response of the instrument to a particle population having a wide distribution of sizes.

It is shown that the particle concentrations measured in channel 1 of the OAP-200Y require correction by a factor which is a function of particle size distribution. For typical experimental situations in rain, the correction factor is approximately 1.8. The remaining size channels do not require correction, provided that the probe sample area and channel width have been properly determined.

1. Introduction

The Optical Array Probe (OAP), developed by Knollenberg (1970, 1972) and produced commercially by Particle Measuring Systems, Inc., of Boulder, Colorado, has proven to be a valuable instrument for measuring the concentrations and size distributions of hydrometeor populations aloft. The OAP is a laser-digital sensor in which the shadow of a particle interrupting a laser beam is focussed at a plane occupied by a photodiode array. The particle size, measured in terms of the number of occulted array elements, is processed and recorded by a digital data acquisition system. These data are used to compute particle concentrations as functions of the size channels determined by the probe logic circuitry.

Some uncertainty has existed concerning the response of an OAP to particles corresponding in size to the lowest three measurement channels. Heymsfield (1976) commented that the OAP-Y suffers from resolution problems in its low size channels. His data, obtained with probes using rectangular or square photodiode elements, occasionally show what appear to be abnormally low values for the recorded count in channel 1 of the precipitation probe. Passarelli (1978) chose to ignore the data from channel 1 of the precipitation probe because of ambiguities in the size interval. Knollenberg (1975) has described undercounting in the lowest three channels of the OAP-200X cloud drop probe and has suggested that this is an effect of sample probability, based on effective depth of field and discrete array element spacing.

Two optical array probes, an OAP-200X cloud drop probe (nominal range 20–300 μm, nominal channel width 20 μm) and an OAP-200Y precipitation probe (nominal range 300–4500 μm, nominal channel width 300 μm), both fitted with circular photodiode elements, have been operated by the Atmospheric Environment Service (AES) as part of an airborne instrumentation package for experiments in cloud seeding techniques (Isaac *et al.*, 1977). Analyses of the data from these experiments and comparison of the OAP-Y results with those of other instruments suggested that the OAP-Y was undercounting significantly at its low end. Specifically, the channel 1 anomaly evident in Heymsfield's (1976) data was also observed in the AES experiments, and a poor match was obtained between the high-resolution end of the cloud-drop probe spectrum and the low-resolution end of the precipitation probe spectrum.

Accordingly, laboratory experiments were carried out in order to clarify the response of the OAP-Y to particles in the size range from 300 to 500 μm. The results of these experiments are presented in this paper.

2. Depth of field considerations

The PMS optical array probes are available in two physical configurations: the X-version has parallel optical extension arms and a sampling aperture of 6.1 cm, while the Y-version has diverging extension arms and an aperture of 26.1 cm. The sample area of an OAP is the product of the effective array width and the depth of field. For N-element OAP's with circular photodetectors and end element rejection, the effective array width is given by

$$Y_{a_i} = dm^{-1}(N-1-i), \tag{1}$$

where d is the photodiode diameter, i denotes the size channel, and m is the overall magnification in the probe receiving optics and is given by

$$m = d/\delta, \tag{2}$$

where δ is the effective channel width.

[1] Present affiliation: Litton Systems Canada Ltd., Rexdale Ontario, Canada.

0021-8952/79/060816-06$05.50

TABLE 1. AES optical array probe sample areas.

Size channel	Effective array width (mm) OAP-X	OAP-Y	Depth of field (mm) OAP-X	(cm) OAP-Y	Sample area (mm²) OAP-X	(cm²) OAP-Y
1	0.403	6.51	0.84	21.9	0.34	14.3
2	0.384	6.22	3.35	26.7*	1.29	16.6
3	0.366	5.92	7.54	26.7*	2.76	15.8
4	0.348	5.62	13.4	26.7*	4.66	15.0
5	0.329	5.33	20.9	26.7*	6.89	14.2
6	0.311	5.03	30.1	26.7*	9.37	13.4
7	0.293	4.74	41.0	26.7*	12.0	12.7
8	0.275	4.44	53.6	26.7*	14.7	11.9
9	0.256	4.14	61.0*	26.7*	15.6	11.1
10	0.238	3.85	61.0*	26.7*	14.5	10.3
11	0.220	3.55	61.0*	26.7*	13.4	9.48
12	0.201	3.26	61.0*	26.7*	12.3	8.69
13	0.183	2.96	61.0*	26.7*	11.2	7.90
14	0.165	2.66	61.0*	26.7*	10.1	7.11
15	0.146	2.37	61.0*	26.7*	8.9	6.32

* Depth of field physically limited by probe aperture.

The effective depth of field for the shadow image of a spherical particle is given by (Knollenberg, 1970)

$$z_f = CD^2(4\lambda)^{-1}, \tag{3}$$

where D is the particle diameter, λ the wavelength of the coherent illumination, and C a constant which depends on the intensity threshold cutoff.

Since the linear extent of the shadow on the sensor array is

$$di = mD, \tag{4}$$

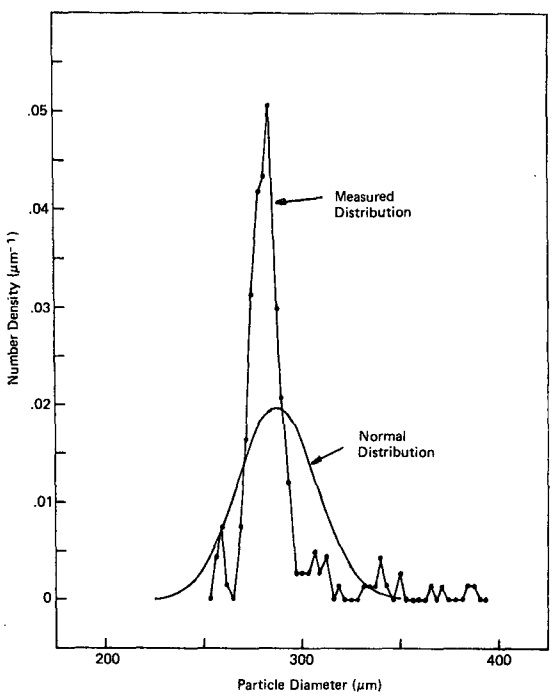

FIG. 1. Size distribution, type 8–16 glass beads, with a normal distribution for comparison. Each distribution has a mean of 288 μm and a standard deviation of 20 μm. Both distributions are normalized.

TABLE 2. Glass bead dimensions.

	Precision			Other	
Bead type	8–16	8–17	8–19	MS-H	MS-XP
Average diameter D (μm)	288	389	558	177	566
Standard deviation SD (μm)	20	40	47	39	97

the sample area can be written

$$A_s = Ci\delta^3(4\lambda)^{-1}(N-1-i). \tag{5}$$

In cases where the optically defined depth of field is larger than the physical aperture of the probe, the latter becomes the limiting factor and (5) is replaced by

$$A_L = L\delta(N-1-i), \tag{6}$$

where L is the length of the finite sampling aperture. This physical limiting of the depth of field occurs within a size channel identified by

$$i_L = \left(\frac{4L\lambda}{C^2\delta}\right)^{\frac{1}{3}}. \tag{7}$$

Sample area calculations for the AES OAP's are summarized in Table 1. It should be noted that in the case of the OAP-Y the depth of field is aperture limited for all channels except channel 1 and that the optically limited depth of field for channel 1 is 82% of the probe aperture.

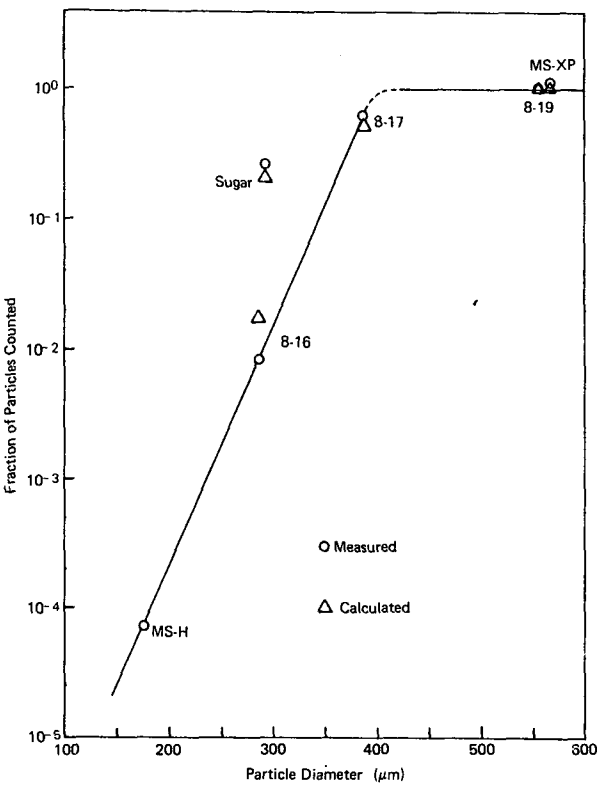

FIG. 2. The response characteristic of the OAP-200Y, showing the measured counting efficiency and that calculated from the known particle size spectra using Eqs. (1).

In the laboratory experiments reported in this paper, care was taken to ensure that virtually all of the particles in the sample being measured passed through the central portion of the sample area. These experimental data are in no manner depth-of-field limited.

3. Laboratory measurements

The probe response measurements were carried out using spherical glass beads to simulate drops of liquid water. Samples of each type of glass bead were optically sized using photomicrographic techniques. A typical size distribution is shown in Fig. 1, along with a normal distribution having the same values of mean and standard deviation. Both distributions are normalized. The precision beads exhibit a size spectrum which is very nearly monodisperse and can be treated as a single line for purposes of computation. Size data on all beads used are given in Table 2.

The OAP-Y is designed for airborne use and, in its particle detection circuitry, incorporates time constants appropriate to particle transit time at aircraft velocities. If a particle passes through the sample area with insufficient speed, the comparator reference voltages begin to collapse and erroneous sizing occurs. To prevent errors caused by low particle velocities, the glass beads were propelled through the sample area from one of several models of a continuously driven air gun. The nozzle of the air gun was positioned so that virtually all of the ejected beads passed through the probe sample area and into a collection tube, making it possible to conduct a series of trials using the same sample of beads. At the normal applied air pressure of 35 kPa, beads having an average diameter of 1.7 mm were ejected at a velocity of 25 m s^{-1}. This is approximately one-third of normal aircraft velocity in the AES experiments and is more than sufficient to prevent undersizing due to reference voltage collapse. By controlling the feed rate of beads to the air gun, it was possible to minimize sizing errors due to particle coincidence, as discussed by Knollenberg (1970).

Small samples of beads were counted out individually using a vacuum-operated small parts handling device, while larger samples were measured volumetrically. Known quantities of glass beads in the size range ~150 to ~600 μm were shot through the sample area and the fraction of beads counted by the probe in each case was recorded. The results, summarized in Fig. 2, indicate that the OAP-Y acts as a high-pass filter having an effective cut-off at ~300 μm.

Curve-fitting and smoothing techniques applied to the data of Fig. 2 resulted in the expressions

$$f(D)=\begin{cases}(3.6\times10^{-8})\exp(0.043D), & D<400\ \mu\text{m}\\ 1.0, & D\geqslant 400\ \mu\text{m}\end{cases} \quad (8)$$

where D is the particle diameter and $f(D)$ the filter function through which the OAP-Y operates on a particle size distribution. Computer calculations were performed in which this filter function was applied to measured glass bead size distributions in order to calculate the counting efficiency

$$F\equiv\int_0^\infty f(D)n(D)dD\approx\int_{1\ \mu\text{m}}^{1000\ \mu\text{m}} f(D)n(D)dD, \quad (9)$$

where $n(D)$ is the optically measured glass bead size distribution, normalized so that

$$\int_0^\infty n(D)dD=1.0. \quad (10)$$

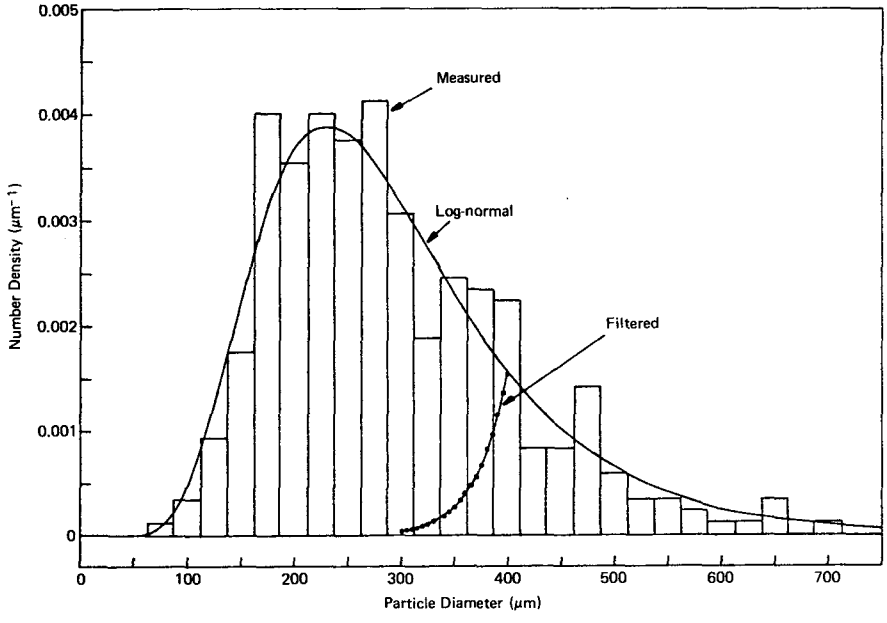

FIG. 3. The size distribution of the sugar crystals.

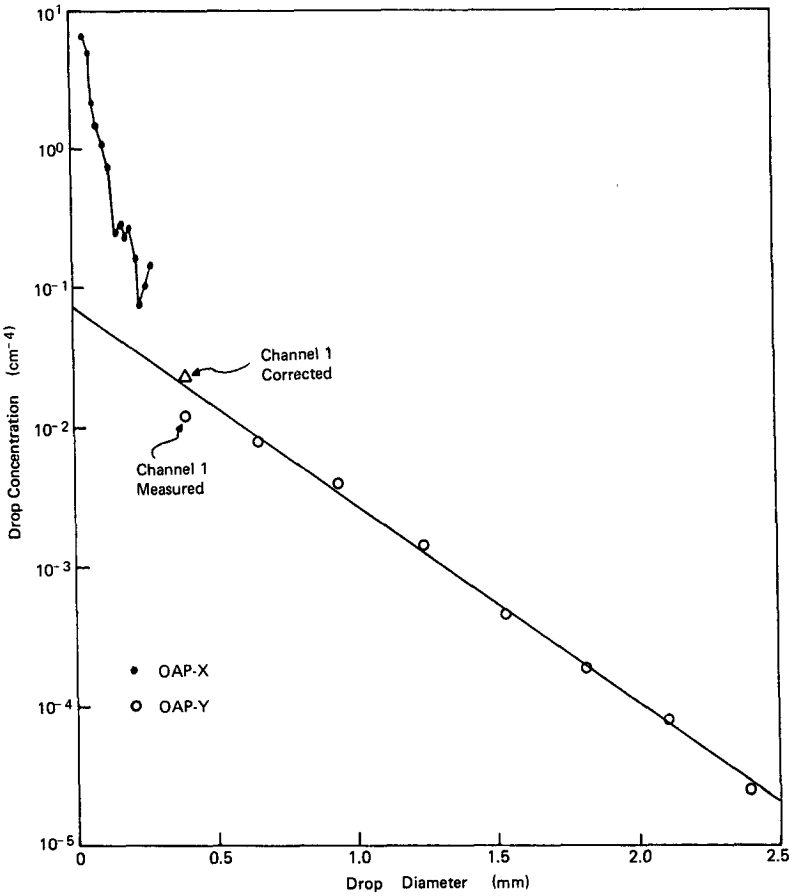

FIG. 4. Raindrop concentrations 2024–2025 GMT 5 July 1976.

The results, shown in Fig. 2, indicate good agreement with the laboratory measurements and suggest that Eqs. (8) provide a realistic description of the low-end characteristics of the OAP-Y.

In the course of laboratory investigations into the behavior of other cloud physics instrumentation, it became necessary to simulate solid hydrometeors with a suitable crystalline particulate. Granulated cane sugar was chosen as an acceptable ice crystal substitute (Schemenauer and Curry, 1979). It is readily available and noncorrosive, has flat crystal faces, and has a range of particle sizes appropriate to the instruments being studied.

As in the case of the glass beads, a sample of sugar crystals was optically sized using photomicrographs. The measured size distribution (Fig. 3) is very nearly log-normal. The histogram of Fig. 3 represents the particle size measured optically, while the smooth curve shows a least-squares-fitted log-normal distribution $N_L(D)$. Also shown in Fig. 3 is the sugar crystal size distribution after filtering by the filter function defined by (8). The fraction of sugar particles which should be counted by the probe is calculated as

$$F=\int_{1\ \mu m}^{1000\ \mu m} f(D)N_L(D)dD=0.22. \tag{11}$$

The measured counting efficiency for sugar is 0.28.

It must be emphasized that the difference in counting efficiency for the sugar sample and the type 8–16 glass beads (Fig. 2) is due to differences in the spectral distributions rather than differences in the physical or optical properties of the particles themselves. The different counting efficiencies result from the fact that the glass beads have size spectra which are nearly monodisperse while the sugar sample contains particles having a wide range of sizes.

It follows that the counting efficiency for channel 1 is very much a function of the properties of the size spectrum of the particle population being sampled. If the statistical properties of the particle distribution are known, the counting efficiency can be computed using Eq. (2). For particle populations having unknown properties, alternate methods are required.

TABLE 3. The OAP-Y channel 1 correction factor as a function of rainfall rate, assuming an exponential drop size distribution.

Rainfall rate (mm h^{-1})	OAP-Y channel 1 correction factor C_1
1	1.883
2	1.839
3	1.817
4	1.802
5	1.792
6	1.784
7	1.777
8	1.772
9	1.767
10	1.763
15	1.748
20	1.739
25	1.732
30	1.727
40	1.718
50	1.713
75	1.703
100	1.696

4. Experimental results

a. General technique

For actual field measurements, the particle concentration is usually a strong function of size, especially for particles $\gtrsim 250$ μm in diameter. The counting efficiency for channel 1 of the OAP-Y therefore varies from one physical situation to another.

A good estimate for the channel 1 counting efficiency can be made by deducing an equation which approximates the particle size distribution as measured by channels 2–15 of the OAP-Y and by any other available instrumentation. This relation is then used to compute a channel 1 correction factor through substitution for $n(D)$ in Eq. (9). The correction factor is then applied to the observed channel 1 particle concentrations before these values are used for the calculation of physical entities, such as radar reflectivity or total liquid water content. The corrected channel 1 particle concentration obtained in this way is more realistic than that obtained by extrapolation of the data in the higher channels, since the latter procedure does not take into account the actual channel 1 measurement.

b. Example

On 5 July 1976 the instrumented aircraft (Isaac *et al.*, 1977) was flown below the base of precipitating cumulus clouds at a flight level of 1600 m and a temperature of +12°C. The average particle concentration observed over a 1 min period is shown in Fig. 4 for both the OAP-X cloud-drop probe and the OAP-Y precipitation probe. Using a least-squares technique, the data in channels 2–15 of the OAP-Y were fitted to an exponential drop size distribution (Marshall and Palmer, 1948)

$$\left.\begin{aligned} N(D) &= N_0 \exp(-\Lambda D) \\ \Lambda &= 41 R^{-0.21}\ [\mathrm{cm}^{-1}] \end{aligned}\right\}, \tag{12}$$

which resulted in the values

$$\left.\begin{aligned} N_0 &= 0.072\ \mathrm{cm}^{-4} \\ R &= 2.92\ \mathrm{mm\ h}^{-1} \end{aligned}\right\}. \tag{13}$$

Using numerical methods, this distribution was used to calculate the channel 1 counting efficiency

$$F_1 = \int_{D_1}^{D_2} N(D) f(D) dD \Big/ \int_{D_1}^{D_2} N(D) dD = 0.55, \tag{14}$$

where D_1 and D_2 are the lower and upper measurement limits of channel 1. For the AES OAP-Y, these are taken as 300 and 500 μm, respectively.

The correction factor for the observed channel 1 particle count is then $C_1 = 1/F_1 = 1.82$. Applying this correction factor to the measured concentration results in the revised value shown in Fig. 4, significantly improving the correlation between the cloud-drop probe and the precipitation probe.

Because C_1 is dependent on the nature of the particle spectrum, it can be expected to vary with rainfall rate. Again assuming the Marshall-Palmer distribution, the values of C_1 shown in Table 3 were computed. It is clear that a correction factor of 1.8 is a reasonable choice for most rainfall situations.

5. Discussion and conclusions

The channel 1 counting efficiency of the precipitation probe can be described in terms of the integrated effect

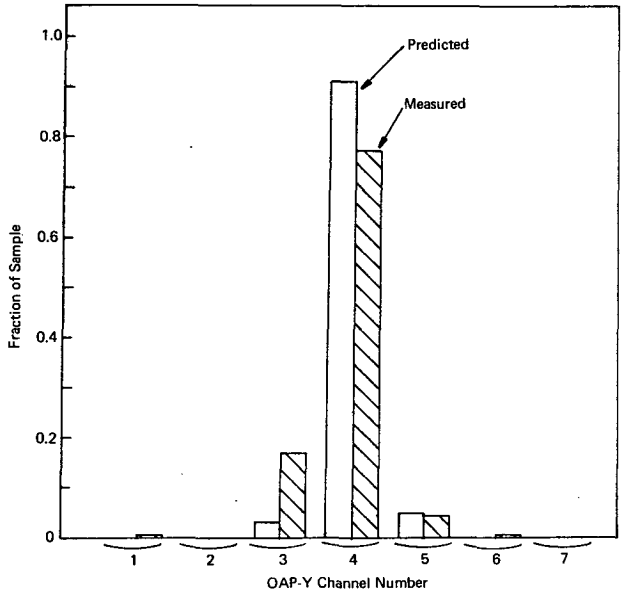

FIG. 5. Size spectrum of type 8–19 glass beads, showing undersizing by the OAP-200Y.

of a filter characteristic which is a strong function of particle size in the range 300–400 μm. If the particle population has an essentially monodisperse size distribution, the channel 1 net counting efficiency is the value of the filter function corresponding to the mean particle size. However, point calculations of counting efficiency seriously underestimate the ability of the probe to count particles when the population contains a broad spectrum of sizes. In this case, the integrated filter technique described above is essential for correct interpretation of the measured particle spectrum.

Particles which are larger than ~400 μm in diameter and which pass through the probe sample volume are certain to be counted, although they may be incorrectly sized. An example of this phenomenon is shown in Fig. 5, which compares the size distribution measured by the OAP-Y with that calculated from the optically measured bead sizes. The net effect, in addition to a slight broadening of the spectrum, is that approximately 10% of the particles which should have been counted in channel 4 were shifted down by one size class.

The effect of this undersizing, thought to be due to the non-zero spacing between elements in the photodiode array, can be minimized by calibrating the probe, in terms of an effective channel width, using precision glass beads having known spectral properties. This method implicitly incorporates a correction factor for the undersizing which occurs during the calibration procedure and reduces to the order of 2% the error in mean particle diameter introduced by such undersizing.

For experimental data, it is necessary to correct the measured channel 1 particle concentrations by making a reasonable assumption concerning the trend of the particle size spectrum in the range from 300–500 μm and computing the appropriate channel 1 correction factor.

Calculations in which such corrected OAP-Y data are compared with measurements obtained using other instruments have shown good agreement (Schemenauer and Curry, 1979; Isaac and Schemenauer, 1978). The channel 1 behavior of the OAP-200Y, as described in this paper, has been repeatedly verified and has been used successfully in the interpretation of data from several years' field experiments. Although the method has not been tested on an X-version precipitation probe or on a cloud-drop probe, it is anticipated that other optical array precipitation probes will exhibit similar behavior.

The high-pass filter characteristic of the OAP-Y precipitation probe was determined from three experimental points, one of which represents a counting efficiency of approximately 10^{-4}, and is evidently subject to variability. The degree of fit shown in Fig. 2 is clearly somewhat fortuitous. Nonetheless, the success which has been obtained by using this function to predict the behavior of the probe when counting sugar crystals suggests that the trend of the filter characteristic is correct.

An OAP array element will respond only to images which result in a 50% reduction in light level. It is for this reason that the response of the probe to spherical particles differs substantially from the response to complex snow crystal forms (Knollenberg, 1975, 1976). Therefore, before applying an OAP-Y channel 1 correction factor to snow crystal data, one must first correct the measured distribution for crystal habit.

As a general rule, for typical values of rainfall rate, the particle concentration measured in channel 1 of the OAP-200Y should be multiplied by a factor of 1.8.

The advantages of the procedure proposed in this paper are that 1) channels 2–15 require no correction, provided that the probe sample area and channel width have been correctly determined, and 2) the integrated filter technique enables a channel 1 correction factor to be computed for each experimental situation.

Acknowledgments. The authors wish to thank the many staff members of the Atmospheric Environment Service (AES) and the Flight Research Facility of the National Aeronautical Establishment (NAE) who assisted in the collection of the aircraft data. The field work was supported by the AES, NAE and the Canadian Forestry Service.

REFERENCES

Heymsfield, A. J., 1976: Particle size distribution measurement: An evaluation of the Knollenberg optical array probes. *Atmos. Tech.*, No. 8, 17–24.

Isaac, G. A., and R. S. Schemenauer, 1978: Large particles in supercooled regions of northern Canadian cumulus clouds. Submitted to *J. Appl. Meteor.*

——, R. S. Schemenauer, C. L. Crozier, A. J. Chisholm, J. I. MacPherson, N. R. Bobbit and L. B. MacHattie, 1977: Preliminary tests of a cumulus cloud seeding technique. *J. Appl. Meteor.*, **16**, 949–958.

Knollenberg, R. G., 1970: The optical array: an alternative to extinction and scattering for particle size measurements. *J. Appl. Meteor.*, **9**, 86–103.

——, 1972: Comparative liquid water content measurements of conventional instruments with an optical array spectrometer. *J. Appl. Meteor.*, **11**, 501–508.

——, 1975: The response of optical array spectrometers to ice and snow: a study of probe size to crystal mass relationships. Particle Measuring Systems, Inc., Boulder, Rep. AFCRL-TR-75-0495, [AFCRL Sci. Rep. No. 1, SCI 75 CO141-9875-001], 70 pp.

——, 1976: The response of optical array spectrometers to ice and snow: A study of 2-D probe area-to-mass relationships. Particle Measuring Systems, Inc., Boulder, Rep. AFGL-TR-76-0273, 31 pp.

Marshall, J. S., and W. McK. Palmer, 1948: The distribution of raindrops with size. *J. Meteor.*, **5**, 165–166.

Passarelli, R. E., Jr., 1978: Theoretical and observational study of snow-size spectra and snowflake aggregation efficiencies. *J. Atmos. Sci.*, **35**, 882–889.

Schemenauer, R. S., and M. J. Curry, 1979: Ice particle/water droplet discrimination with an optical ice particle counter. *J. Appl. Meteor.*, **18**, 215–224.